DMD Fast Forward. Published on January 28, 2008 as doi:10.1124/dmd.107.018655
This article has not been copyedited and formatted. The final version may differ from this version.

Identification of a Novel Glucosylsulfate Conjugate as a Metabolite of ARQ 501 (ß-lapachone) in Mammals

Ronald E. Savage, Andrew N. Tyler[1], Xiu-Sheng Miao[2] and Thomas C. K. Chan

Department of Preclinical Development and Clinical Pharmacology, ArQule Inc.

Woburn, Massachusetts (R.E.S., A.N.T., X-S.M., T.C.K.C.)

DMD Fast Forward. Published on January 28, 2008 as DOI: 10.1124/dmd.107.018655
This article has not been copyedited and formatted. The final version may differ from this version.

Running title page

a) Running Title: Novel Glucosylsulfate Metabolite of ß-lapachone in Mammals

b) Corresponding author

Ronald E. Savage, PhD

ArQule, Inc.

19 Presidential Way, Woburn, MA 01801

Tel: (781) 994-0428

Fax: (781) 287-8147

Email: ***rsavage@arqule.com***

c) Number of text pages: 12

Number of tables: 2

Number of figures: 6

Number of schemes: 0

Number of references: 29

Number of words in the *Abstract*: 157

Number of words in the *Introduction*: 510

Number of words in the *Discussion*: 831

d) Abbreviations used are: HPLC, high performance liquid chromatography; LC/MS, liquid chromatography/mass spectrometry; MS/MS mass spectrometry/mass spectrometry; LC/NMR, liquid chromatography/ nuclear magnetic resonance, HPβCD, hydroxypropyl-β-cyclodextrin; IP, intraperitoneal; IV, intravenous; Q-Tof, quadrupole-time-of-flight; ES, electrospray; UGTs, UDP-glucuronyosyltransferases; SULTs,

sulfotransferases; GSTs, glutathione S-transferases; UDPGA, UDP-glucuronic acid; GlcNAc, N-acetylglucosamine; βGlcA, β-glucuronic acid

Abstract

ARQ 501 (3, 4-dihydro-2,2-dimethyl-2H-naphtho [1,2-*b*]pyran-5,6-dione) is a fully synthetic version of the natural product β-lapachone which has been isolated from the lapacho tree (*Tabebuia impetiginosa* or *Tabebuia avellanedae*) and has demonstrated promising anti-cancer activity. ARQ 501 formulated with hydroxypropyl-β-cyclodextrin (HPβCD) has successfully completed phase I clinical trials and is currently in several phase II human clinical trials for the treatment of pancreatic cancer, head and neck cancer, and leiomyosarcoma. The metabolites of ARQ 501 were investigated by low-resolution and high-resolution mass spectrometry in plasma from (nu/nu) mice, rats, and humans treated with the compound. The data for one of the metabolites identified are consistent with conjugation of ARQ 501 with a glucosylsulfate moiety (m/z 241; fragment ion). While other glucosylsulfate conjugates have been identified as metabolites of pesticides in cotton plants and in crustaceans as phase II metabolites of pyrenes, none has been previously identified in mammals. Data reported here identify a novel metabolic pathway for humans.

Introduction

ARQ 501 (Figure 1) is an investigational anticancer agent that consists of a fully synthetic small molecule (3,4-dihydro-2,2-dimethyl-2H-naphtho[1,2-*b*]pyran-5,6-dione, ß-lapachone, molecular weight 242 daltons) in a stable HPβCD formulation suitable for intravenous administration. In pre-clinical studies *in vitro* (Docampo et al., 1979; Schaffner-Sabba et al., 1984; Chau et al., 1998; Li et al., 2000) and *in vivo* (Li et al., 1999; Ough et al., 2005), ARQ 501 showed activity against a variety of cancers. In a phase Ib clinical study, ARQ 501 showed promising anticancer activity against pancreatic cancer when administered in combination with gemcitabine. ARQ-501 is currently in several Phase II cancer trials.

Most pharmaceutical products (~ 80%) that undergo biotransformation are cleared by the phase I cytochrome P450 enzymes (Coughtrie et al., 2003). However, it is widely known that a second class of enzymes, the phase II enzymes, also plays a significant role in drug metabolism. Among the most common phase II enzymes are the UDP-glucuronosyltransferases (UGTs), the sulfotransferases (SULTs) and the glutathione S-transferases (GSTs). Phase II metabolites are easily identified by mass spectrometry as these biotransformation pathways are well-characterized and the metabolites easily predicted by looking for mass differences when comparing the parent drug to its metabolite. For example, glucuronide, sulfate, and glutathione metabolites are easily predicted by an increase in mass of 176 Da, 80 Da and 305 Da respectively, to the mass of the parent drug (Kostianen et al., 2003; Levsen et al., 2005). Over the last decade, highly sensitive and specific analytical techniques such as LC/MS/MS, high resolution quadrupole-time-of-flight (Q-Tof) mass spectrometry, and LC/NMR have been widely

applied to the study of drug metabolism. Not surprisingly, this has led to the recent discovery of a number of novel metabolites (Jaggi et al., 2002; Miao et al., 2005; Chang et al., 2006; Endo et al., 2007) and in some cases, to the discovery of novel metabolic pathways (Tang et al., 2003; Yin et al., 2003; Zhen et al., 2006).

Although many studies have been conducted on ß-lapachone (ARQ 501), there have been no previous reports on its metabolism either in animals or in humans. Preliminary metabolism studies for this compound were conducted with plasma from mice dosed IP and rats dosed IV at 40 mg/kg with ARQ 501 formulated with HPβCD. Later analyses were performed with human plasma samples obtained from a clinical study. In all species, the majority of conjugated product corresponds to glucuronidation or sulfation, but one metabolite representing a minor proportion of conjugate does not correspond to any commonly expected phase II metabolic process. The present study was conducted to characterize this rare metabolite, which has been identified as a novel glucosylsulfate conjugate. There are several accounts of a similar metabolic process occurring in cotton plants that were exposed to pesticides including profenofos (Capps et al., 1996) and 2,4-dichlorophenoxyacetic acid (Laurent et al., 2000). More recently (Ikenaka et al., 2007), glucosylsulfate conjugates have been identified as new phase II metabolites in aquatic crustaceans exposed to pyrenes. To our knowledge, glucosylsulfate conjugates have not yet been reported in mammals until now.

Materials and Methods

Chemicals and Reagents. ARQ 501 was synthesized by ArQule, Inc. HPβCD was obtained from Cargill, Inc. (Minneapolis, MN). Acetonitrile and HPLC grade water were purchased from EMD Chemicals (Gilbbstown, NJ). β-Glucuronidase type IX-A was purchased from Sigma-Aldrich (St Louis, MO). All other chemicals were of reagent grade or better.

Dosing and plasma collection. Nude mice (nu/nu) were obtained from Charles River Laboratories, Inc. (Wilmington, MA). Mice were dosed at 40 mg/kg by intraperitoneal injection with ARQ 501 formulated in 40% HPβCD. Blood collected 30 minutes following injection was used for this study. The blood was collected into a container containing sodium EDTA and centrifuged for 10 minutes at 3000g at ambient temperature. The plasma fraction was removed, frozen over dry ice, and then stored at -80ºC until analyzed.

Analysis of clinical samples. A volume of 100 µL human plasma collected at the 8 hour time point from a patient dosed with 140 mg/m^2 of ARQ 501 in 40% HPβCD was deproteinized with 3 volumes of acetonitrile and centrifuged for 10 minutes at 3000g at ambient temperature. The supernatant was dried down with gentle nitrogen stream and reconstituted to 100 µL with acetonitrile/water (25/75). A Waters Atlantis dC18 column (150×2.1mm, 3µ; Waters Corp, Milford, MA) was used for chromatographic separation. The mobile phase solvents were water (A) and acetonitrile (B) both modified with 0.1% formic acid. The applied gradient was as follows: solvent B started at 25% and held for 1 min, linearly increased to 54% B from 1 to 23 min, held at 54% B for 3 min, then

increased from 54% to 95% B over 2 min, and maintained at 95% B for 4 min, finally back to 25% B at 33 min and allowed to equilibrate.

Glucuronidase Assay. β-Glucuronidase type IX-A was dissolved in aqueous ammonium acetate (100 mM, pH 6.8) to obtain an enzyme activity of 5500 units/mL. Plasma aliquots (200 µL) from blood taken at 0.25 hour post-dose were combined with aqueous ammonium acetate (100 mM, pH 6.8) and β-Glucuronidase solution (100 µL). The mixture was incubated for 1 hour at 37ºC with gentle agitation. After 1 hour, the reaction was stopped by the addition of 500 µL of acetonitrile. Supernatant from the centrifuged reaction mixture was evaporated to dryness and then reconstituted in 100 µL of acetonitrile/water (50:50) for LC/MS analysis.

Metabolite Identification. Plasma aliquots (50 µL) were combined with 100 µL of acetonitrile, centrifuged and the supernatant removed for LC/MS analysis.

Low-resolution mass spectrometry was performed using a Quattro Ultima triple quadrupole mass spectrometer (Waters Corp., Milford, MA) equipped with an Agilent 1100 binary pump liquid chromatography system (Agilent, Palo Alto, CA) and a LEAP auto injector (LEAP Technologies, Carrboro, NC). Chromatography was performed on a Phenomenex Jupiter C18 column (150 x 2.1 mm, 5 micron particle size; Phenomenex Inc., Torrance, CA) using water modified with 0.1% formic acid as the aqueous phase and acetonitrile modified with 0.1% formic acid as the organic phase. The applied gradient was as follows: solvent B started at 10% B and held for 0.5 min, linearly increased to 95% B from 0.5 to 13 min, held at 95% B for 0.5 min, finally back to 10% B at 13.6 min and allowed to equilibrate.

High-resolution MS was performed using a Q-Tof mass spectrometer (Waters Corp., Milford, MA) equipped with an Agilent 1100 pump modified for low flow chromatography and an Agilent low volume auto injector. Identical buffers were used for both LC/MS studies. Chromatography was performed on a Phenomenex Jupiter C_{18} column (150 x 2.1 mm, 5 micron particle size; Phenomenex Inc., Torrance, CA) using water modified with 0.1% formic acid as the aqueous phase and acetonitrile modified with 0.1% formic acid as the organic phase. The gradient applied was the same as described above. Ion trap mass spectrometry was performed using a LTQ XL™ linear ion trap (Thermo Scientific, Inc.). MS^n mass spectra were collected by running the Data Dependent™ function in negative-ion mode. Sample separation was conducted on a Hypersil Gold column (100 × 2.1 mm, 1.9μm) using water (A) and acetonitrile (B) both modified with 0.1% formic acid. The applied gradient was as follows: solvent B started at 10% B and held for 0.5 min, linearly increased to 60% B from 0.5 to 30 min, then to 95% at 35 min, held at 95% B for 5 min, finally back to 10% B at 40.5 min and allowed to equilibrate before the next run.

Results

Identification of Metabolite 1. Examination of the negative-ion electrospray LC/MS data from mouse plasma extracts revealed a molecular anion peak $(M-H)^{-1}$ at m/z 485 for metabolite 1 that was not observed in the data obtained from the baseline plasma extracts of pre-dose animals (Figure 2). As seen in Figure 2, two other metabolites of ARQ 501, a glucuronide (m/z 419) and a sulfate (m/z 323) are shown to provide a qualitative comparison of retention times and ion intensity. Subsequent MS/MS analysis of the m/z 485 peak produced a spectrum dominated by fragments at m/z 243 and m/z 187 (Figure 3). These fragments are identified, respectively, as the anion of reduced ARQ 501 (m/z 243) and the loss of butene (C_4H_8) from the C-ring of the m/z 243 ion to give m/z 187. The presence of these conserved fragment ions help to confirm the peak as a metabolite of ARQ 501. These same fragments are also the most intense fragments observed in the product ion spectra for the glucuronide and sulfate metabolites of ARQ 501. Incubation of plasma extracts with glucuronidase enzyme does not affect the intensity of the peak of metabolite I over a one hour time period (Figure 4), while the signals corresponding to glucuronidation of reduced ARQ 501 were completely eliminated (data not shown). Additionally, the area of the ARQ 501 peak (not shown) increased by almost 6 fold indicating that glucuronidation of ARQ 501 might be a major metabolic pathway. Similar experiments with sulfatase resulted in a several fold increase of the ARQ 501 peak area however, despite attempting a number of different incubation conditions, complete conversion of the conjugated sulfate peak to ARQ 501 could not be attained.

The mass of the metabolite 1 anion (m/z 485) and the calculated mass of reduced ARQ 501 (m/z 243) are different by 242 mass units. The product ion spectrum of m/z

485 shows a peak at m/z 405 which results from a neutral loss of 80 mass units. Subsequently, an additional neutral loss of 162 mass units is observed from m/z 405 to m/z 243. These neutral loss masses are consistent with either a phosphate or sulfate group (loss of 80 mass units) and a glucose residue (loss of 162 mass units). The fragment ion m/z 97 corresponds to either hydrogen sulfate anion HSO_4^- or dihydrogen phosphate anion $H_2PO_4^-$, while the ion at m/z 80 (SO_3^-) indicates that a sulfate group is most likely attached to the molecule. The fragment ion observed at m/z 241 corresponds to the anion of the entire conjugation moiety. The absence of m/z 323 in the product ion mass spectrum of m/z 485 indicates that glucose is attached directly to ARQ 501 as an inner part the conjugate moiety. Figure 3b shows the MS/MS spectrum of metabolite 1 generated using ion trap mass spectrometry. This spectrum depicts a more prominent fragment ion of m/z 241 in addition to the m/z 405 fragment ion and the m/z 485 parent ion. Subsequent MS^3 fragmentation (Figure 3c) of the m/z 241 ion clearly shows the presence of the m/z 97 fragment (HSO_4^-or $H_2PO_4^-$) and the m/z 80 fragment (SO_3^-). These data provide further support that the sulfate (or phosphate) group is attached to the glucose portion of the molecule.

The proposed phosphate and sulfate entities were distinguished by exact mass measurement, using high-resolution mass spectrometry. As shown in Table 1, the calculated mass for the anion of the phosphate species $[C_{21}H_{26}PO_{11}]^-$ = 485.1213 m/z, while the calculated mass for the sulfate species $[C_{21}H_{25}O_{11}S]^-$ = 485.1116 m/z. The measured mass for the metabolite anion was 485.1102 m/z, which has a deviation of 0.0111 masses (22.8 ppm) from the expected mass of the phosphate form and a deviation of 0.0014 mass units (2.9 ppm) from the expected mass of the sulfate form. The measured

deviation for the former exceeds the expected maximum experimental error of ± 10 ppm; therefore the data are consistent with the sulfate form.

Additional evidence for sulfation is obtained from inspection of the isotopic distribution of the molecular signal. The natural presence of the ^{34}S isotope gives a 4% enhancement to the intensity of the (p+2) isotope peak compared with the expected intensity of that peak if a monoisotopic phosphorous atom were present. Table 1 compares the measured isotope peak ratios for the molecular anion peak with the theoretical ratios for the phosphorylated and sulfated species. Again, the data are consistent with the sulfated form.

The exact masses of the product ions from m/z 485 are summarized in Table 2, which compares the measured masses with the calculated masses for the hypothetical compositional assignments for the major ions. The measured masses are all consistent with the proposed structures.

Figure 5 demonstrates the identified glucuronide, sulfate and glucosylsulfate conjugate metabolite peaks in a human clinical sample, and two regioisomers (at position 5 and 6) are observed for each of these metabolic pathways.

Discussion

Metabolite 1 was identified as a glucosylsulfate conjugate attached to either the C_5 or C_6 (Figure 1) carbon atom of ARQ 501. All of the major conjugation metabolites of ARQ 501 arise from a two-step process, which requires reduction of the B-ring of ARQ 501 to a hydroxyquinone, followed by conjugation at the reduced site. While reduction is required as a first step, we have been unable to find any evidence for the free hydroxyquinone in plasma samples from subjects dosed with ARQ 501. The redox cycling properties of ß-lapachone are well known (Villamil et al., 2004). The reduction potential of ß-lapachone to the hydroxyquinone is pH dependent and has been reported as -0.116 V at pH 4.5 (Abreu et al., 2002); under *in vivo* conditions it appears that the hydroxyquinone is either rapidly conjugated or oxidized back to the ketone. Reduction of ß-lapachone and subsequent reaction with mercaptoethanol have shown that these adducts are unstable and revert back to ß-lapachone (Oliveira-Brett et al., 2002).

We believe this is the first report of glucosylsulfate conjugation as a metabolic pathway in mammals and we have observed this metabolite in the plasma of mice, rats, and humans after dosing with ARQ 501. A similar metabolic process has been identified for the insecticide profenofos (Capps et al., 1996) and for 2, 4-dicholorphenoxyacetic acid (Laurent et al., 2000) when applied to cotton plants. As discussed by Capps and coworkers, profenofos is primarily metabolized in cotton plants to the glucose conjugate of 4-bromo-2-chlorophenol. However, identification of an early eluting more polar metabolite via HPLC analysis led to the discovery of the glucosylsulfate conjugate of 4-bromo-2-chlorophenol. In this metabolite, the glucose moiety is sulfated at the C_6 position. Laurent and coworkers discovered a similar glucosylsulfate metabolite (also in

cotton plants) when the plants were treated with 2, 4-dicholorphenoxyacetic acid. This metabolite was identified as 2,4-dichlorophenol-(6-O-sulfate)-glucoside. The product ion spectrum of this metabolite produced the same m/z 241 fragment ion corresponding to the sulfated glucose which we have observed in the product ion spectrum of the glucosylsulfate conjugate of ARQ 501. Hence, this fragment appears to be a marker for glucosylsulfate conjugation just as the 175 m/z and 113 m/z fragment ions are specific markers for glucuronide conjugation (Kostiainen et. al., 2003; Kuuranne et. al., 1999). This is an important observation given that we have been unable to obtain any NMR data for this metabolite primarily due to the synthetic difficulties in preparing an authentic standard which are centered around the instability of reduction products of ARQ 501.

The only other report of glycosylsulfate metabolites in plants involves the metabolism of phenmedipham in sugar beets to 2-O-sulfate glucosides (Lamoureux, 1989). Hence, even in plants, reports of glucosylsulfate conjugates are rare. There has been a recent report of glucosylsulfate conjugates of 1-hydroxypyrene as phase II metabolites in crustaceans (Ikenaka et al., 2007). Identification of this metabolite was based on the glucosylsulfate marker fragment ion of 241 m/z which was present in the negative electrospray product ion spectrum of the parent molecule.

Although somewhat uncommon, there have been several reports of glucoside conjugates of endogenous compounds and drugs in mammals including mice and dogs (Duggan et al., 1974 and Boberg et al., 1998). In some reported cases, O-β-D-glucosides were the preferential and may be the only metabolites formed (Chemla et al., 2001 and Nakano et al., 1986). Tang et al. (2003) recently reported the presence of both a glucuronide and glucoside metabolite of an endothelin ET_A receptor antagonist in assay

incubations employing human liver microsomes. These studies also demonstrated that the glucuronyl transferase UGT2B7 was responsible for the formation of both metabolites showing that UGT2B7 can use both UDPGA and UDPG as cosubstrates. It was further suggested that glucosidation may be an alternate metabolic route when levels of UDPGA are exhausted by detoxification via the primary metabolic route. Interestingly, in the biosynthesis of heparin sulfate, glucoside conjugation occurs via the enzymes GlcNAc transferase II and βGlcA transferase II followed by sulfation which occurs at various positions in the polysaccharide chain including the C_6 position in which sulfation is catalyzed by glucosaminyl, 6-O-sulfotransferase (Strott, 2002). Whether sulfation occurs before or after glucosidation for ARQ 501 metabolite 1 is currently under investigation.

In conclusion, these results demonstrate that a glucosylsulfate conjugate of ARQ 501 is a metabolite in plasma samples of animals and humans dosed with ARQ 501 (Figure 6). Based on previous reports (Capps et al., 1996; Ikenaka et al., 2007), we suspect that the glucose is sulfated at the C_6 position of the glucosylsulfate conjugate however in the absence of NMR data a definitive identification cannot be made. Additionally, in the absence of ^{14}C data and synthetic standards it is difficult to quantitatively assess the contribution of this novel pathway relative to the total metabolism of ARQ 501. Efforts to clarify the structure of the glucoslylsulfate metabolite of ARQ 501 and the biological significance of this novel metabolic pathway in the clearance of ARQ 501 in mammals are ongoing.

Acknowledgements

We gratefully acknowledge Dr. Allen Annis of Schering-Plough Pharmaceuticals for his technical assistance with exact mass measurements.

References

Abreu FC, Goulart MOF, and Brett AMO (2002) Reduction of lapachones in aqueous media at a glassy carbon electrode. *Electroanalysis* **14**:29-34.

Boberg M, Angerbauer R, Kanhai WK, Karl W, Kern A, Radtke M, and Steinke W (1998) Biotransformation of cerivastatin in mice, rats, and dogs in vivo. *Drug Metab Dispos* **26**:640-652.

Capps TM, Barringer VM, Eberle WJ, Brown DR, and Sanson DR (1996) Identification of a unique glucosylsulfate conjugate metabolite of profenofos in cotton. *J Agric Food Chem* **44:**2408-2411.

Chang Y, Moody DE, and McCance-Katz EF (2006) Novel metabolites of buprenorphine detected in human liver microsomes and human urine. *Drug Metab Dispos* **34**:440-448.

Chau YP, Shiah SG, Don MJ, and Kuo ML (1988) Involvement of hydrogen peroxide in topoisomerase inhibitor ß-lapachone-induced apoptosis and differentiation in human leukemia cells. *Free Radic Biol Med* **24**:660-670.

Chemla Z, Vesely J, Lemr K, Rypka M, Hanus J, Havlicek L, Krystof V, Michnova L, Fuksova K, and Lukes J (2001) In vivo metabolism of 2,6,9-trisubstituted purine-derived cylin-dependent kinase inhibitor bohemine in mice: Glucosidation as the principal metabolic route. *Drug Metab Dispos* **29**:326-334.

Coughtrie MWH, and Fisher MB (2003) Drug metabolizing enzymes: Cytochrome P450 and other enzymes in drug discovery and development (Lee SJ, Obach RS, and Fisher MB eds) pp 541-575, CRC Press, Taylor and Francis Group, Boca Raton.

Docampo R, Cruz FS, Boveris A, Muniz RP, and Esquivel DM (1979) ß-lapachone enhancement of lipid peroxidation and superoxide anion and hydrogen peroxide formation by sarcoma 180 ascites tumor cells. *Biochem Pharmacol* **28**:723-728.

Duggan DE, Baldwin JJ, Arison BH, and Rhodes RE (1974) N-glucoside formation as a detoxification mechanism in mammals. *J Phamacol Exp Ther* **190**:563-569.

Endo T, Ban M, Hirata K, Yamamoto A, Hara Y, and Momose Y (2007) Involvement of CYP2A6 in the formation of a novel metabolite, 3-chydroxypilocarpine, from pilocarpine in human liver microsomes. *Drug Metab Dispos* **35**:476-483.

Ikenaka I, Ishizaka M, Eun H, and Miyabara Y (2007) Glucose-sulfate conjugates as a new phase II metabolite formed by aquatic crustaceans. *Biochem Biophys Res Commun* **360**:490-495.

Jaggi R, Addison RS, King AR, Suthers BD, and Dickinson RG (2002) Conjugation of desmethylnaproxen in the rat-a novel acyl glucuronide-sulfate diconjugate as a major biliary metabolite. *Drug Metab Dispos* **30**:161-166.

Kostiainen R, Kotiaho T, Kuuranne T, and Auriola S (2003) Liquid chromatography/atmospheric pressure ionization-mass spectrometry in drug metabolism studies. *J. Mass Spectrom* **38**:357-372.

Kuuranne T, Mikko V, Leinonen A, and Kostiainen R (2000) Electrospray and atmospheric pressure chemical ionization tandem mass spectrometric behavior of eight anabolic steroid glucuronides. *J Am Soc Mass Spectrom* **11**:722-730.

Lamoureux GL (1989) Plant metabolism of herbicides in relation to detoxification, selectivity, antidosing, and synergism, in Xenobiotic Metabolism and Disposition

(Kato R, Estabrook RW, and Gayen MN eds) pp 267-274, Taylor and Francis, Bristol.

Laurent F, Debrauwer L, Rathahao E, and Scalla R (2000) 2,4-Dichlorophenoxyacetic acid metabolism in transgenic tolerant cotton (Gossypium hirsutum). *J Agric Food Chem* **48**:5307-5311.

Levsen K, Schiebel H-M, Behnke B, Dotzer R, Dreher W, Elend M, and Thiele H (2006) Structure elucidation of phase II metabolites by tandem mass spectrometry: An overview. *J Chromatogr A* **1067**:55-72.

Li CJ, Li Y-Z, Pinto AV, and Pardee AB (1999) Potent inhibition of tumor survival in vivo by ß-lapachone plus taxol: Combining drugs imposes different artificial checkpoints. *Proc Natl Acad Sci* USA **96**:13369-13374.

Li Y, Li CJ, Yu D, and Pardee AB (2000) Potent induction of apoptosis by beta-lapachone in human multiple myeloma cell lines and patient cells. *J Mol Med* **6:**1008-1015.

Miao Z, Kamel A, and Prakash C (2005) Characterization of a novel metabolite intermediate of ziprasidone in hepatic cytosolic fractions of rat, dog, and human by ESI-MS/MS, hydrogen/deuterium exchange, and chemical derivatization. *Drug Metab Dispos* **33**:879-883.

Nakano K, Ohashi M, and Harigaya S (1986) The β-glucosidation and β-glucuronidation of pantothenic acid compared with p-nitrophenol in dog liver microsomes. *Chem Pharm Bull* **34**:3949-3952.

Oliveira-Brett AM, Goulart MO, and Abreu FC (2002) Reduction of lapachones and their reaction with L-cysteine and mercaptoethanol on glassy carbon electrodes. *Bioelectrochemistry* **56**:53-5.

Ough M, Lewis A, Bey EA, Gao J, Ritchie JM, Bornmann W, Boothman DA, Oberley LW, and Cullen JJ (2005) Efficacy of ß-lapachone in pancreatic cancer treatment. *Cancer Biol & Thera*. **4**:95-102.

Schaffner-Sabba K, Schmidt-Ruppin KH, Wehrli W, Schuerch AR, and Wasley JW (1984) ß-lapachone: Synthesis of derivatives and activities in tumor models. *J Med Chem* **27**:990-994.

Strott CA (2002) Sulfonation and Molecular Action. *Endocr Rev* **23**:703-732.

Tang C, Hochman JH, MA B, Subramanian R, and Kamlesh PV (2003) Acyl glucuronidation and glucosidation of a new and selective endothelin ET_A receptor antagonist in human liver microsomes. *Drug Metab Dispos* **31**:37-45.

Villamil SF, Stoppani AOM, and Dubin M (2004) Redox cycling of ß-lapachone and structural analogues in microsomal and cytosol liver preparations. *Methods Enzymol* **378**:67-87.

Yin W, Doss GA, Stearns RA, Chaudhary AG, Hop CE, Franklin RB, and Kumar S (2003) A novel P450-catalyzed transformation of the 2,2,6,6-tetramethyl piperidine moiety to a 2,2-dimethyl pyrrolidine in human liver microsomes: characterization by high resolution quadrupole-time-of-flight mass spectrometry and ^{1}H-NMR. *Drug Metab Dispos* **31**:215-223.

Zhen Y, Slanar O, Krausz KW, Chen C, Slavik J, Mcphail K, Zabriskie TM, Perlik F, Gonzalez FJ, and Idle JR (2006) 3,4-Dehydrodebrisoquine, a novel debrisoquine

metabolite formed from 4-hydroxydebrisquine that affects the CYP2D6 metabolic ratio. *Drug Metab Dispos* **34**:1563-1574.

Footnote page

[1]Current address: Novartis Institutes for Biomedical Research, 100 Technology Square, Cambridge, Massachusetts.

[2]Current address: Eli Lilly and Company, Lilly Corporate Center, Indianapolis, Indiana.

Legends for Figures

FIG. 1. Structure of ARQ 501 (ß-lapachone).

FIG. 2. A, Overlay of extracted ion $(M-H)^{-1}$ chromatograms of 1) ARQ 501 glucosylsulfate m/z 485, 2) ARQ 501 glucuronide m/z 419, and 3) ARQ 501 sulfate m/z 323 obtained from 0.5 hour post-dose mouse sample. B, Overlay of the same extracted ion chromatograms as in Figure 2A obtained from a pre-dose mouse sample.

FIG. 3. A, Product ion mass spectrum (triple quadrupole) from the molecular anion peak $(M-H)^{-1}$ at m/z 485. B, Product ion mass spectrum (ion trap) from the molecular anion peak $(M-H)^{-1}$ at m/z 485. C, MS^3 spectrum (ion trap) of m/z 241 fragment ion.

FIG. 4. Extracted ion chromatograms of glucosylsulfate peak (m/z 485) from plasma samples incubated with (bottom trace) and without (top trace) β-glucuronidase.

FIG. 5. Overlay of extracted ion $(M-H)^{-1}$ chromatograms of selected metabolites from a human clinical plasma sample.

FIG. 6. Proposed metabolic pathway in the formation of β-lapachone glucosylsulfate, glucuronide, and sulfate.

DMD Fast Forward. Published on January 28, 2008 as DOI: 10.1124/dmd.107.018655
This article has not been copyedited and formatted. The final version may differ from this version.

Table 1. Comparison of measured relative abundance of molecular anion isotope peaks with calculated values for theoretical phosphorylated and sulfated forms.

m/z	% Calc. Abundance - Sulfate form	% Calc. Abundance - Phosphate form	Measured Abundance
485.1	100.0	100.0	100.0
486.1	25.0	24.2	26.8
487.1	9.6	5.0	11.0
488.1	1.9	0.0	2.3

Table 2. Comparison of calculated and measured masses for the major fragments observed in the product ion mass spectrum for metabolite I.

COMPOSITION						
C	**H**	**O**	**S**	Calc. Mass	Meas. Mass	Diff / mmu
11	7	3		187.0395	187.0458	6.3
6	9	8	1	241.0018	241.0040	2.2
15	15	3		243.1020	243.1033	1.3
21	25	8		405.1548	405.1487	-6.1
21	25	11	1	485.1116	485.1102	-1.4

DMD Fast Forward. Published on January 28, 2008 as DOI: 10.1124/dmd.107.018655
This article has not been copyedited and formatted. The final version may differ from this version.

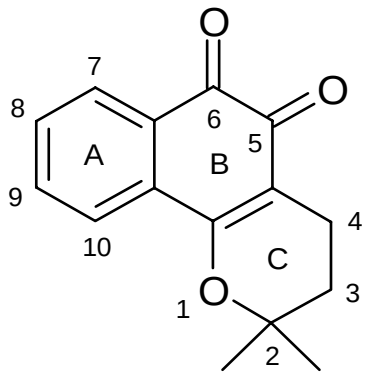

Fig 1

DMD Fast Forward. Published on January 28, 2008 as DOI: 10.1124/dmd.107.018655
This article has not been copyedited and formatted. The final version may differ from this version.

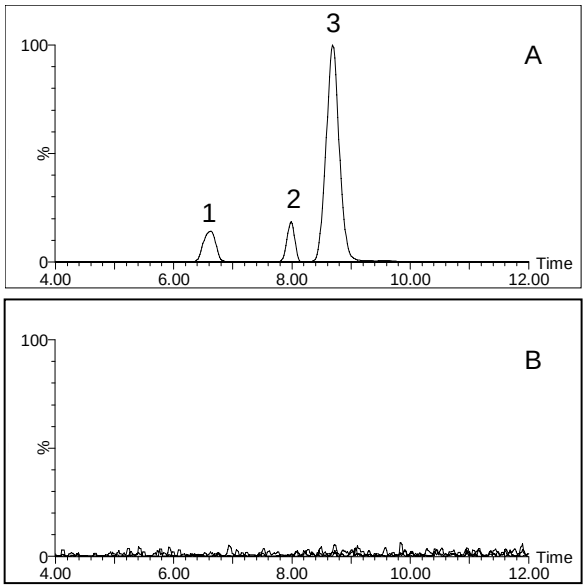

Fig 2

DMD Fast Forward. Published on January 28, 2008 as DOI: 10.1124/dmd.107.018655
This article has not been copyedited and formatted. The final version may differ from this version.

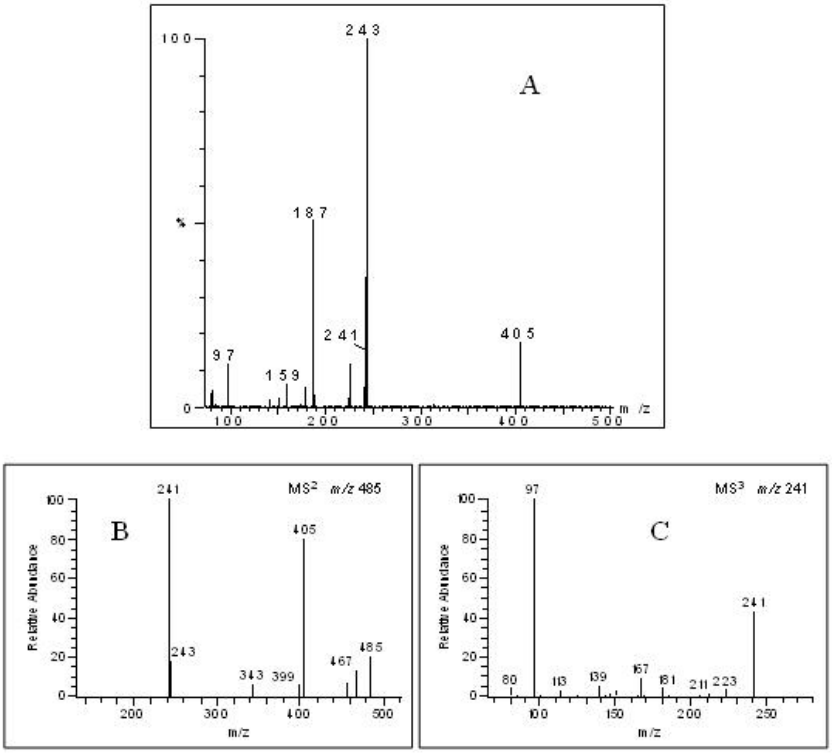

Fig 3

DMD Fast Forward. Published on January 28, 2008 as DOI: 10.1124/dmd.107.018655
This article has not been copyedited and formatted. The final version may differ from this version.

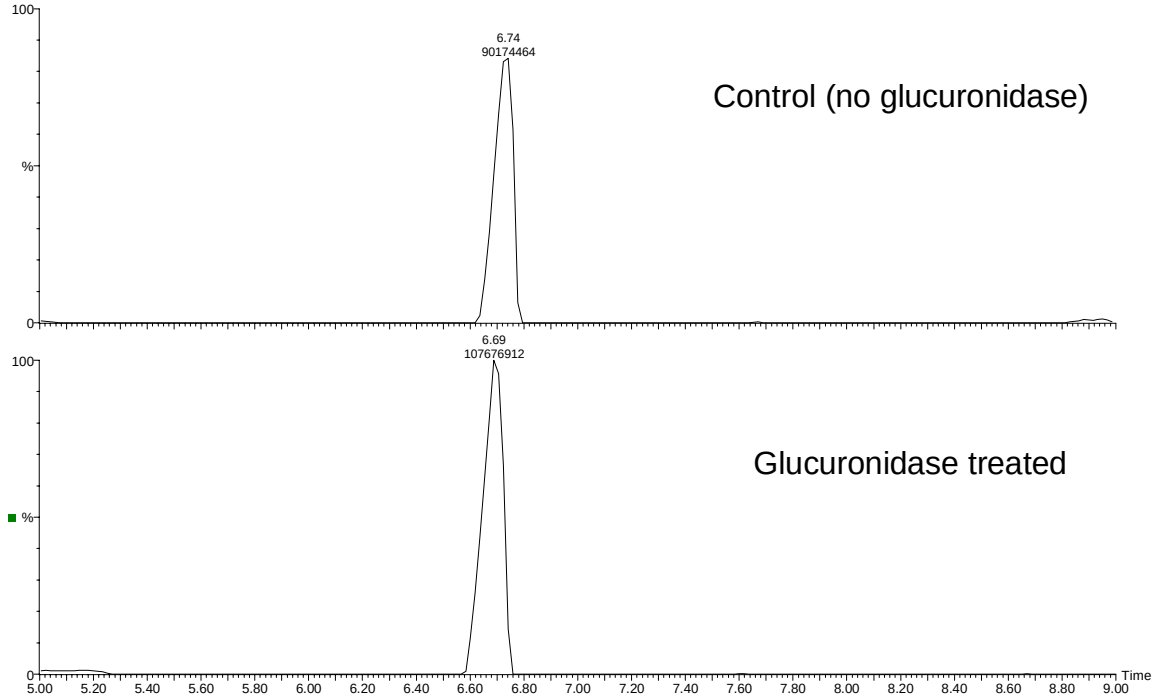

Fig 4

DMD Fast Forward. Published on January 28, 2008 as DOI: 10.1124/dmd.107.018655
This article has not been copyedited and formatted. The final version may differ from this version.

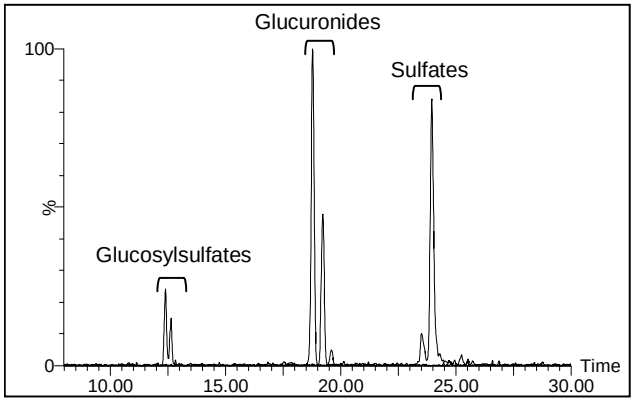

Fig 5

DMD Fast Forward. Published on January 28, 2008 as DOI: 10.1124/dmd.107.018655
This article has not been copyedited and formatted. The final version may differ from this version.

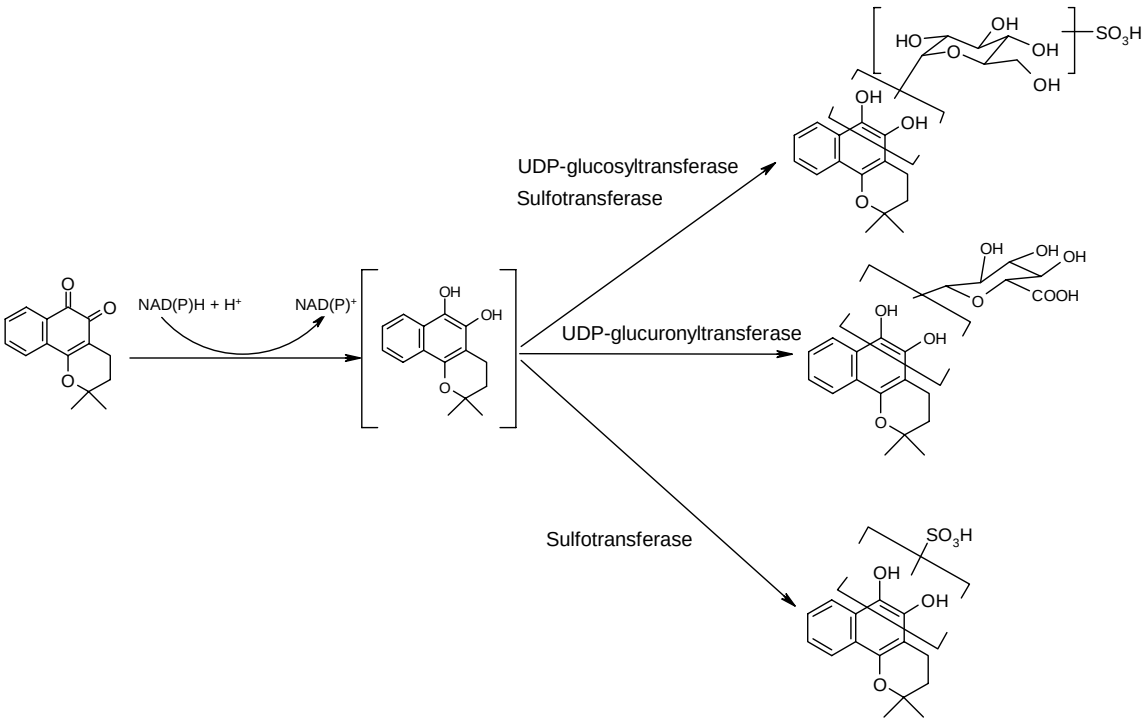

Fig 6